

Visual-Based Forklift Learning System Enabling Zero-Shot Sim2Real Without Real-World Data

Koshi Oishi^{*,1}, Teruki Kato¹, Hiroya Makino¹, and Seigo Ito¹

This work has been submitted to the IEEE for possible publication. Copyright may be transferred without notice, after which this version may no longer be accessible

Abstract—Forklifts are used extensively in various industrial settings and are in high demand for automation. In particular, counterbalance forklifts are highly versatile and employed in diverse scenarios. However, efforts to automate these processes are lacking, primarily owing to the absence of a safe and performance-verifiable development environment. This study proposes a learning system that combines a photorealistic digital learning environment with a 1/14-scale robotic forklift environment to address this challenge. Inspired by the training-based learning approach adopted by forklift operators, we employ an end-to-end vision-based deep reinforcement learning approach. The learning is conducted in a digitalized environment created from CAD data, making it safe and eliminating the need for real-world data. In addition, we safely validate the method in a physical setting utilizing a 1/14-scale robotic forklift with a configuration similar to that of a real forklift. We achieved a 60% success rate in pallet loading tasks in real experiments using a robotic forklift. Our approach demonstrates zero-shot sim2real with a simple method that does not require heuristic additions. This learning-based approach is considered a first step towards the automation of counterbalance forklifts.

I. INTRODUCTION

Forklifts are essential in various industries, including factories, logistics centers, ports, and construction sites. In particular, counterbalance forklifts are central to the industry owing to their robustness and power, generating significant demand for automation. Recent advancements have led to the automation of reach type forklifts, considering their low power requirements and high maneuverability [1]. In contrast, automating counterbalance forklift operations requires advanced controllers that can leverage the versatility and overcome the limited maneuverability of forklifts. As humans learn these tasks through training, applying deep reinforcement learning (DRL) to automation is a natural progression [2], [3], [4]. However, research on its application to forklifts remains limited, likely owing to the risks of conducting experiments in real environments and the lack of training datasets. Therefore, a learning system that can overcome these challenges is required.

DRL has issues such as the dangers of real-world training and low sample efficiency. A common strategy for these issues is sim2real, in which a policy is trained in a digital environment and transferred to the real world [5]. However, learning in a digital environment creates a new challenge

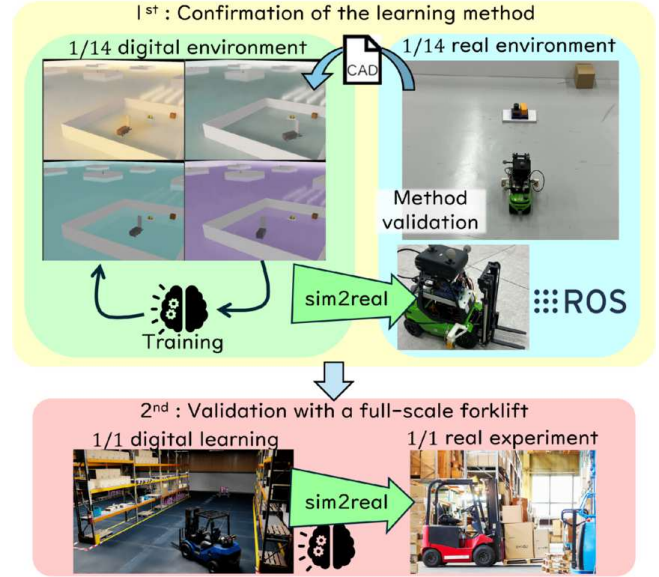


Fig. 1: Proposed concept. To implement deep reinforcement learning-based control on a full-scale forklift, we first test sim2real in a smaller environment. Sim2real is applied to the full-scale forklift after confirming the safety of the method.

known as the domain gap. Various methods have been proposed to bridge this gap. However, methods that do not rely on real-world data are preferable for forklifts, as collecting failure data poses significant challenges. Notable studies without real-world data include those focusing on soccer and mountain climbing with bipedal and quadrupedal robots, respectively [6], [7]. These studies used domain randomization, which randomizes the environment during training [8], [9]. However, the use of visual information in these studies is limited. Moreover, as opposed to these small-scale robots, the first validation of a sim2real method using large machines such as forklifts carries risks, even though safety is verified in the digital environment.

We propose a practical learning system for automating counterbalance forklifts in pallet loading tasks involving pallet approach and loading decision. In pallet approach, a policy is optimized using end-to-end DRL to control the forklift based on same visual and velocity information as humans operators. A loading decision policy to perform a loading task is acquired through supervised learning. Our concept involves training and validation in 1/14-scale digital and real environments and subsequent extension of the learning method to full scale after confirming the safety in these

¹ The authors are with Toyota Central R&D Labs., Inc., 41-1, Yokomichi, Nagakute, Aichi, Japan.

* Corresponding author. e1616@mosk.tytlabs.co.jp

environments, as shown in Fig. 1. Furthermore, to address the domain gap in which real-world data is lacking, we use domain randomization with NVIDIA Omniverse Isaac Sim (Isaac Sim), which is a highly advanced photorealistic digital environment [10]. Constructing this digital environment requires only CAD data, thereby eliminating the need for real-world data in training. Moreover, the 1/14-scale forklift used in the real environment features front-wheel drive and rear-wheel steering, similar to the full-scale version, and its lift function operates hydraulically. We developed the 1/14 scale forklift using a robot operating system (ROS) [11]. This study represents the first step towards the learning-based control of real counterbalance forklifts. The contributions of our research are as follows:

- We propose a forklift learning system using a photorealistic digital environment that allows for safe research and validation.
- We introduce an end-to-end DRL method for vision-based forklift control that focus on pallet approach, which does not require real-world data.
- We develop a method for dataset construction for the pallet loading decision policy using a photorealistic digital environment.
- We demonstrate zero-shot sim2real using a 1/14-scale forklift.

The remainder of this paper is organized as follows. Related works are introduced in Section II. Section III presents the target tasks and learning setup for the proposed system. Our proposed learning system that uses a photorealistic simulator is described in Section IV. Section V outlines the demonstration in the real environment. Finally, concluding remarks and future directions are presented in Section V.

II. RELATED WORK

Research on the automation of counterbalance forklifts has been limited to date. Walter et al. [12] and Teller et al. [13] focused on non-learning-based methods that use multiple LiDAR sensors for environmental perception. However, to the best of our knowledge, few studies have explored real-world implementations of the automation of counterbalance forklifts. Hadwiger et al. [14] conducted DRL using visual inputs on a counterbalance forklift in a digital environment. However, their method lacked sufficient handling of the domain gap issue and was only evaluated on the digital.

End-to-end DRL, which acquires policies through training in a manner similar to human learning, can achieve human-like performance [2], [3]. Trained human operators play a central role in operating counterbalance forklifts, contributing to the adoption of the end-to-end DRL method. Common tasks in DRL applications include navigation and dexterous manipulation [5], [15]. Forklifts require both navigation and dexterous operation because the forks are directly attached to the wheels. In previous research, navigation and manipulation were handled by a robot arm mounted on a mobile platform, which differs from our task, as dexterous manipulation is performed by the arm [16].

DRL has been studied extensively in sim2real scenarios because of the dangers associated with real-world experimentation and the low sample efficiency of such experiments [5], [8], [17], [18]. Domain randomization is an effective method for addressing the domain gap in sim2real without relying on real-world data, and it has been widely used in many studies [8], [19], [20], [21]. Among these, the research closest to ours is the study on soccer, which requires both navigation and dexterous manipulation [6]. Similar to our method, this research progressed to the stage of performing soccer tasks using low-cost onboard cameras [22]. However, they employed NeRF to achieve vision-based tasks, thereby negating the advantage of not using real-world data, which was a key strength in previous studies [23]. Furthermore, although NeRF is effective for static visuals, it is not well suited to moving objects such as pallets or loads [24].

Recent advancements have made it possible to create photorealistic digital environments in which human training can be performed using VR headsets [25]. Mittal et al. [10] and Yu et al. [26] proposed photorealistic learning systems using Isaac Sim. While these studies used the photorealistic digital environment to generate datasets for supervised learning, they did not report on vision-based DRL. Our study leverages the photorealism of Isaac Sim and domain randomization to address the zero-shot sim2real of vision-based DRL that does not require real-world data and can adapt to dynamic environments.

III. VISION-BASED FORKLIFT CONTROL VIA DRL

This section first describes the targeted tasks, followed by the learning setup employed by our learning system. The goal is to develop a forklift controller that can perform forklift tasks. This study emphasizes the overall learning framework, including the practical implementation; therefore, we use simple methods for training.

A. Target task

The target task is the pallet loading operation by a forklift. It involves randomly positioning the forklift within the visible range of the pallet and then executing the loading process. We divide this task into two phases: the approach to the pallet and lifting operation. Different policies are applied to each phase. We use a simple decision policy to determine whether to lift the pallet. Therefore, the focus is on the learning method related to the forklift-specific approach to the pallet. The observation data used for this task include visual and velocity information, similar to that used by a human operator. In addition, forklift operators lean to the sides to check the alignment between the forks and pallets. Therefore, we installed two cameras on the left and right sides of the forklift to capture images of the forks and pallets.

B. Policy design for pallet approach

The approach policy is designed to output the throttle and steering of the forklift based on the visual and velocity inputs obtained from the camera images and velocity data, respectively. The camera images, which are 352×288 RGB

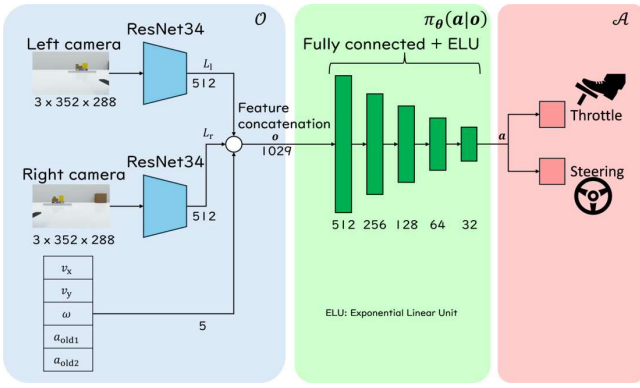


Fig. 2: Approach policy design.

images, are first resized to 224×224 . The resized images are then converted into feature vectors, $L_l \in \mathbb{R}^{512}$ and $L_r \in \mathbb{R}^{512}$, using a ResNet pretrained on ImageNet [27], [28]. These feature vectors are subsequently used as inputs for the policy. This method was proposed as Resnet as representation for reinforcement learning [29]. No special processing is required because we use a standard pretrained ResNet without domain adaptation. In addition, assuming that speed sensors are installed, we utilize the two-dimensional speed information $\mathbf{v} := [v_x, v_y]^T$ and yaw rate ω . Finally, we include the past actions a_{old1} and a_{old2} . Thus, the observation space \mathcal{O} is a 1029-dimensional vector space.

The policy network $\pi_{\theta}(\mathbf{a}|\mathbf{o})$ outputs the normalized throttle and steering commands for the forklift. Here, $\mathbf{a} \in \mathcal{A} = [-1, 1]^2$ represents the actions and θ denotes the parameters of the policy network. The network $\pi_{\theta}(\mathbf{a}|\mathbf{o})$ consists of five fully connected layers with exponential linear units as activation functions. The overall structure is shown in Fig. 2.

C. Training method

We use the on-policy reinforcement learning algorithm proximal policy optimization (PPO) to train the approach policy $\pi_{\theta}(\mathbf{a}|\mathbf{o})$ [30]. The following subsections describe the loss and reward functions employed in our method.

1) *Loss function*: The actor and critic networks share a common network, which is optimized using the following single loss function:

$$L_t(\theta) = \mathbb{E}_t \left[L_t^{\text{PPO}}(\theta) + c_1 L_t^{\text{value}}(\theta) - c_2 H(\pi_{\theta}(\cdot|\mathbf{o}_t)) + c_3 L_t^{\text{bound}}(\theta) \right], \quad (1)$$

where $L_t^{\text{PPO}}(\theta)$ denotes the loss of the PPO policy, $L_t^{\text{value}}(\theta)$ denotes the state-value loss, $H_t(\pi_{\theta}(\cdot|\mathbf{o}_t))$ denotes the entropy, $L_t^{\text{bound}}(\theta)$ denotes the boundary loss, and c denotes the weight. Moreover, $L_t^{\text{PPO}}(\theta)$ is determined by

$$L_t^{\text{PPO}}(\theta) = -\mathbb{E}_t \left[\min(\rho_t(\theta)\hat{A}_t, \text{clip}(\rho_t(\theta), 1 - \varepsilon, 1 + \varepsilon)\hat{A}_t) \right], \quad (2)$$

$$\rho_t(\theta) = \frac{\pi_{\theta}(\mathbf{a}_t|\mathbf{o}_t)}{\pi_{\theta_{old}}(\mathbf{a}_t|\mathbf{o}_t)},$$

where the clip function smooths the gradients by limiting the loss changes and ε denotes the clipping parameter. In addition, \hat{A}_t is computed using generalized advantage estimation [30]. Furthermore, $L_t^{\text{value}}(\theta)$ is obtained by

$$L_t^{\text{value}}(\theta) = \mathbb{E}_t \left[\left(V_{\theta}(\mathbf{s}_t) - V_t^{\text{target}} \right)^2 \right], \quad (3)$$

where $V_{\theta}(\mathbf{s}_t)$ denotes the state-value function, V_t^{target} denotes the target state-value function, and \mathbf{s}_t denotes the state of the environment, including privileged information. In addition, the entropy is introduced to encourage exploration, as follows:

$$H(\pi_{\theta}(\cdot|\mathbf{o}_t)) = -\sum_{\mathbf{a}} \pi_{\theta}(\mathbf{a}|\mathbf{o}_t) \log \pi_{\theta}(\mathbf{a}|\mathbf{o}_t). \quad (4)$$

Finally, the boundary loss L_{bound} is introduced to prevent the actions from taking excessively large values:

$$L_t^{\text{bound}}(\theta) = \|\boldsymbol{\mu}(\mathbf{o}_t)\|, \quad (5)$$

where $\boldsymbol{\mu}(\mathbf{o}_t)$ denotes the mean vector of the actions output by the policy $\pi_{\theta}(\cdot|\mathbf{o}_t)$.

2) *Reward function*: Our reward function consists of positive and penalty rewards for desirable and undesirable states, respectively. In addition, calculating these rewards uses states of privileged information available in the digital environment. For the positive rewards, the deviation from a reference trajectory is used. The initial position is the location of the forklift at the start of the task, and the terminal position is the pallet. The reference trajectory is based on the approximation of a clothoid curve, which remains fixed throughout the task. The positive reward R_+ is defined as follows:

$$R_+ = \alpha_1 \frac{1}{r_d} + \alpha_2 \frac{1}{r_{cd}} + \alpha_3 \frac{1}{r_{c\psi}} + \alpha_4 r_g, \quad (6)$$

where r_d and r_{cd} are the distances from the center of the forks to the pallet and clothoid curve, respectively, $r_{c\psi}$ is the difference between the orientation of the forks and the tangent to the clothoid curve, $r_g \in \{0, 1\}$ is a special reward assigned when the forks reach the pallet position, and α represents the weight. The components of R_+ are illustrated in Fig. 3.

Unlike general navigation tasks, our task requires inserting the forks without moving the pallet. Therefore, the penalty rewards are defined as follows:

$$R_- = \alpha_5 r_p + \alpha_6 r_v + \alpha_7 r_a + \alpha_8 r_{ini}, \quad (7)$$

where

$$r_p = \begin{cases} -1 & \text{if } \|\mathbf{v}_p\| > 0.01, \\ 0 & \text{otherwise,} \end{cases}$$

$$r_v = \begin{cases} -(\|\mathbf{v}\| - 0.05)^2 & \text{if } \|\mathbf{v}\| < 0.05, \\ 0 & \text{otherwise,} \end{cases}$$

$$r_a = -\|\mathbf{a} - \mathbf{a}_{old}\|^2,$$

$$r_{ini} = \begin{cases} -1 & \text{if } \|\mathbf{v}\| < 0.05 \text{ and } r_d > 0.3, \\ 0 & \text{otherwise,} \end{cases}$$

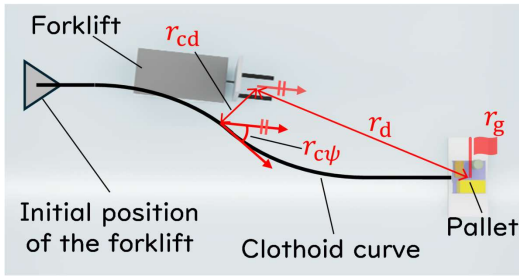


Fig. 3: State used for calculating R_+ .

TABLE I: Domain randomization targets

Item	Range
Observed speed	$\pm 10\%$ of value
Action	$\pm 10\%$ of command
Floor color	$\pm 20\%$ RGB
Pallet stand color	$\pm 20\%$ RGB
Pallet and load color	$\pm 20\%$ RGB
Light intensity	100–100000 lm
Light temp.	2000–7500 K

where \mathbf{v}_p is the velocity of the pallet and \mathbf{a}_{old} is the previous action. r_p is the penalty for contacting the pallet; a negative reward is assigned if the pallet starts to move. r_v and r_a are penalties designed to bridge the gap between the digital and real environments. Specifically, r_v prevents excessive speed, whereas r_a prevents the actions from becoming erratic. r_{ini} is a penalty to prevent the forklift from freezing at the initial position. Therefore, the reward function can be summarized as follows:

$$R = R_+ + R_- \quad (8)$$

IV. FORKLIFT LEARNING SYSTEM

Learning-based controls often have black-box characteristics, making it challenging to validate them in high-powered, contact-heavy industrial machinery. Therefore, we constructed digital and real environments at a 1/14 scale. The digital environment was created using Isaac Sim, which supports the development of photorealistic environments [10]. We leveraged the extensive randomization capabilities and parallel learning features of the tool to address the domain gap challenges of reinforcement learning. The real environment was constructed using a ROS [11].

A. Digital and real environment

We constructed digital and real environments for the task involving approaching a pallet within a 1.8m square space. The appearances of the digital and real environments are shown in Fig. 4.

The forklift was randomly placed within the green triangle shown in Fig. 4a and made to approach the pallet. This task relied on visual input; however, the forklift did not appear in the camera field of view. Therefore, the forklift design in the digital environment was simplified. The objects in the digital environment were created using CAD data and specifications, without any real-world image capture.

As reflections are known to affect visual navigation in real environments negatively, fluorescent lights were modeled and placed as shown in Fig. 4c [31]. The 1.8m space was enclosed by white walls in the digital and real environments. The critical dimensions, namely the sizes of the pallet and forklift, are shown in Fig. 4f. The specifications of the forklift are discussed in the following section. Isaac Sim allowed for various randomizations within this digital environment. The information that was randomized in this study is listed in Table I. Examples of the floor and lighting randomization are shown in Fig. 5.

B. Real forklift

For the real-world environment, we modified a 1/14 scale forklift from LESU, which is a China-based manufacturer [32]. The dimensions of this forklift were 100×310 mm, and the forks measured 75×10 mm. This forklift, similar to counterbalance forklifts, featured front-wheel drive and rear-wheel steering. In addition, the lift and tilt functions of the fork were powered by hydraulics.

All computers installed on this forklift were replaced with a Raspberry Pi 4 single-board computer to implement the ROS. Raspberry Pi received action \mathbf{a} , calculated by the ground control computer based on the approach policy $\pi_{\theta}(\mathbf{a}|\mathbf{o})$, and transmitted these commands to the respective servos and motors via the servo driver board, as shown in Fig. 6. Two USB cameras were connected to the Raspberry Pi; the captured images were sent to the ground control computer as observation data. The cameras were mounted on both sides of the forklift, as shown in Fig. 4f, and were equipped with OV5640 sensors and 60-degree field-of-view lenses.

Velocity information was obtained using a motion capture system. Note that only velocity information was used in our method. The position data were only used for experimental evaluation. All control processes were executed at 15 Hz.

C. Digital forklift

The forklift in the digital environment was implemented with a simplified design, as mentioned in Section IV-A. The drivetrain components were operated using the Articulations-based controllers of Isaac Sim. The parameters of these controllers were configured to match the speed response of the real forklift to the command inputs closely.

D. DRL on Isaac Sim

We used “OmniIsaacGymEnvs,” a parallel learning framework that is based on “rl_games” and available in Isaac Sim [33], [34]. This tool allows for constructing multiple environments on the same ground plane, improving the sampling efficiency. The randomization of the colors for pallets and other objects was handled independently for each environment for domain randomization. We synchronized task resets and shared the values for lighting and floor color randomization across all environments to simplify the implementation.

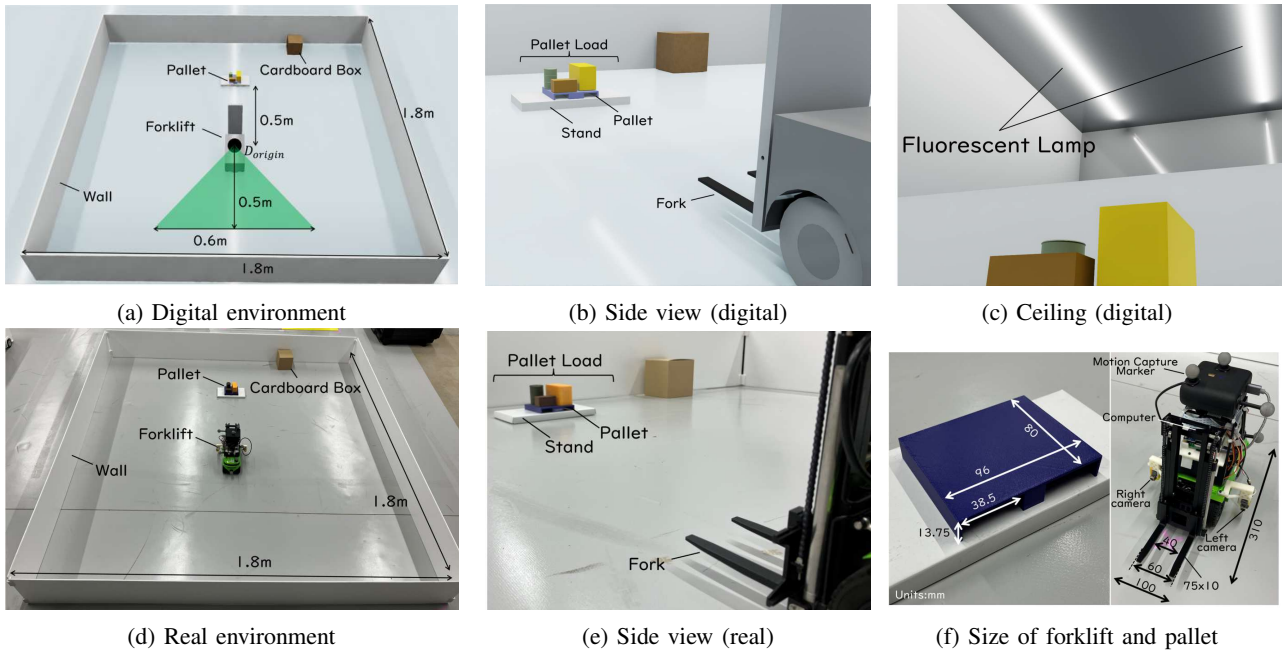


Fig. 4: Digital and real environments. (a), (b), and (c) represent the digital environment. The green triangle in (a) indicates the initial position of the forklift, which is randomly determined at the start of the task. D_{origin} denotes the origin. (d) and (e) represent the real environment. (f) represents the size of the real forklift and pallet. Units are in mm.

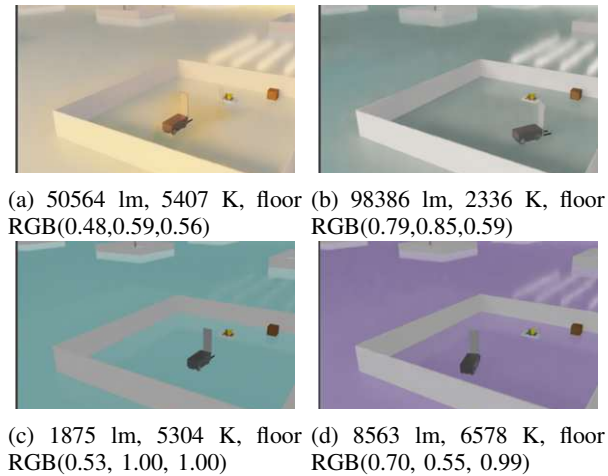


Fig. 5: Example of domain randomization.

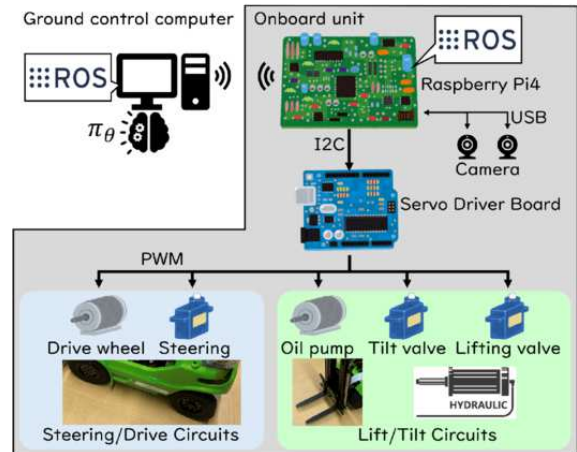


Fig. 6: Real forklift control system.

E. Decision policy for loading

To perform loading, it is crucial to verify that the approach to the pallet has been successful. In this study, we designed a decision policy that activates when the forklift is stationary. The decision policy determines whether to lift the forks after the forklift approaches the pallet using the approach policy obtained through DRL. This policy was trained using binary classification through supervised learning. The training dataset was generated by collecting camera images from successful and unsuccessful attempts within the Isaac Sim environment, as shown in Fig. 7. Consequently, no real-world data were used to create this dataset.

V. REAL DEMONSTRATION

This section presents the results of deploying our method in a real environment. As our method employs zero-shot sim2real, the policies trained in the digital environment was directly transferred to the real environment without any modifications.

A. Setup

We trained the policies in the digital environment described in Section IV using the method outlined in Section III. The ground control computer with 96 GB of RAM, an Intel® Xeon™ Gold 6146 3.2 GHz processor, and an NVIDIA RTX A6000 was used. The task was performed

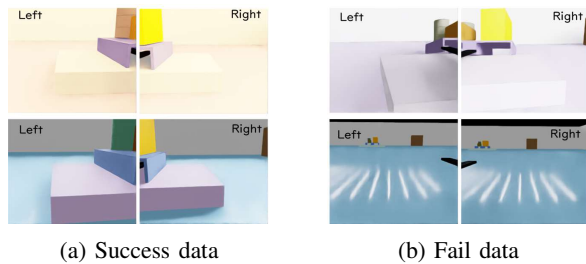


Fig. 7: Dataset for decision policy.

TABLE II: Demonstration results

	ours	Man A	Man B	Man C
Success rate (%)	60	50	40	90
Time (s)	6.5	7.7	17.2	24.5

by positioning the forklift within a triangular area, similar to that during the training in the digital environment, as shown in Fig. 4. In this demonstration, we repeatedly positioned the forklift at an initial position, directed it to approach the pallet, and manually returned it to a new starting position after each task.

The decision policy for determining whether to lift the forks was triggered 3s after the forklift came to a stop. In the case of a successful decision of approach, the forklift followed a sequence of actions: lifting the forks, reversing, and lowering the forks to unload the pallet. Successful completion of the task was dependent on executing the sequence without dropping the pallet load.

We compared the results of our method with those of human-operated trials to demonstrate the difficulty of the task. Human operators controlled the forklift using a joystick, relying on the same camera images and velocity information as the approach policy. Before the experiment, the operators were provided with a brief explanation and a 3-min practice session. As hydraulic operation requires experience, the experiment was considered successful if the operator could insert the forks at least two-thirds into the pallet.

B. Results

We performed the task 10 times with our learned policies and the three human operators. The success rates and average times of the pallet approach required for success are shown in Table II. The average success rate for human operators was 60% and the completion time was 16.5 s. Although Man C achieved a success rate of 90%, he employed a cautious driving technique, repeatedly stopping and checking the camera images frequently. This indicates that the task was not straightforward. Our method achieved a 60% success rate on the pallet approach task at the highest speed. Figure 8 shows the position and velocity of the forklift forks with our method during the 10 trials based on the motion capture system. This result suggests that our approach policy learned efficient behavior, accelerating initially and decelerating near the pallet. Furthermore, the success rate of loading decisions was 90%. This decision error occurred once when the forks

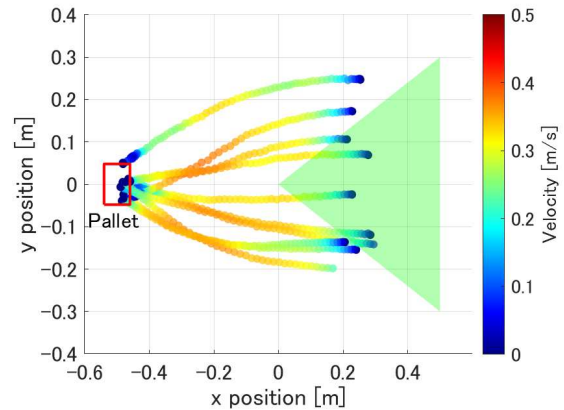


Fig. 8: Trajectory and velocity of the center of the fork. The green triangle indicates the range of randomized initial positions during digital training. As the trajectory represents the path of the fork, the center of the forklift body is positioned 0.2m further back.

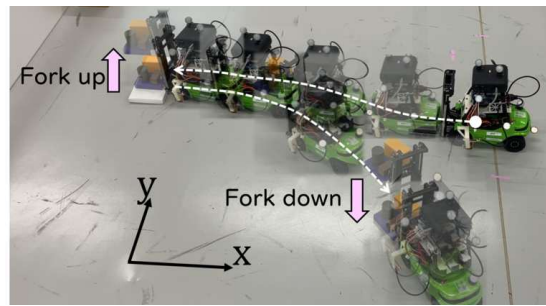


Fig. 9: Demonstration of forklift task.

were inserted only on one side. Snapshots of a successful attempt are presented in Fig. 9.

Our method could produce a controller for forklift tasks using only visual and velocity data, similar to human operation, although the performance was not ideal. Furthermore, the experiment was safe and easy to conduct.

VI. CONCLUSIONS AND FUTURE WORK

We have proposed a learning system for a counterbalance forklift to perform pallet loading tasks using only cameras and velocity data. In addition, we developed a 1/14-scale forklift with the same configuration as the 1/1-scale one. The forklift allows us to validate the trained policies for safety. Moreover, our method eliminates reliance on real-world data by utilizing a photorealistic environment and domain randomization. Our approach policy achieved a 60% success rate through efficient behavior in loading tasks in real-world experiments. Additionally, using a decision policy learned from a dataset constructed with a digital environment, the forklift could perform loading tasks based on the success or failure of its approach to the pallet. These policies were implemented through zero-shot sim2real, requiring no heuristic adjustments. Based on these results, this study presented a practical method for applying learning-

based control to counterbalance forklifts, offering significant potential to advance automation across various industries.

Future research will focus on improving the accuracy using the results of various existing studies and validating the findings on a full-scale forklift. In addition, as a higher-level task, we will explore integrating control systems and task allocation strategies to automate forklift tasks fully.

REFERENCES

- [1] Linde Material Handling, “Automation for your warehouse.” [Online]. Available: <https://www.linde-mh.com/en/Solutions/Intralogistics-Automation>
- [2] V. Mnih, K. Kavukcuoglu, D. Silver, A. A. Rusu, J. Veness, M. G. Bellemare, A. Graves, M. Riedmiller, A. K. Fidjeland, G. Ostrovski *et al.*, “Human-level control through deep reinforcement learning,” *nature*, vol. 518, no. 7540, pp. 529–533, 2015.
- [3] S. Levine, C. Finn, T. Darrell, and P. Abbeel, “End-to-end training of deep visuomotor policies,” *Journal of Machine Learning Research*, vol. 17, no. 39, pp. 1–40, 2016.
- [4] E. Kaufmann, L. Bauersfeld, A. Loquercio, M. Müller, V. Koltun, and D. Scaramuzza, “Champion-level drone racing using deep reinforcement learning,” *Nature*, vol. 620, no. 7976, pp. 982–987, 2023.
- [5] W. Zhao, J. Queraltá, and T. Westerlund, “Sim-to-real transfer in deep reinforcement learning for robotics: a survey,” in *2020 IEEE Symposium Series on Computational Intelligence (SSCI)*, 2020, pp. 737–744.
- [6] T. Haarnoja, B. Moran, G. Lever, S. Huang, D. Tirumala, J. Humplik, M. Wulfmeier, S. Tunyasuvunakool, N. Siegel, R. Hafner, M. Bloesch, K. Hartikainen, A. Byravan, L. Hasenclever, Y. Tassa, F. Sadeghi, N. Batchelor, F. Casarini, S. Saliceti, C. Game, N. Sreendra, K. Patel, M. Gwira, A. Huber, N. Hurlley, F. Nori, R. Hadsell, and N. Heess, “Learning agile soccer skills for a bipedal robot with deep reinforcement learning,” *Science Robotics*, vol. 9, 2024.
- [7] T. Miki, J. Lee, J. Hwangbo, L. Wellhausen, V. Koltun, and M. Hutter, “Learning robust perceptive locomotion for quadrupedal robots in the wild,” *Science Robotics*, vol. 7, 2022.
- [8] J. Tobin, R. Fong, A. Ray, J. Schneider, W. Zaremba, and P. Abbeel, “Domain randomization for transferring deep neural networks from simulation to the real world,” in *2017 IEEE/RSJ International Conference on Intelligent Robots and Systems (IROS)*, 2017, pp. 23–30.
- [9] X. B. Peng, M. Andrychowicz, W. Zaremba, and P. Abbeel, “Sim-to-real transfer of robotic control with dynamics randomization,” in *2018 IEEE International Conference on Robotics and Automation (ICRA)*, 2018, pp. 3803–3810.
- [10] M. Mittal, C. Yu, Q. Yu, J. Liu, N. Rudin, D. Hoeller, J. Yuan, R. Singh, Y. Guo, H. Mazhar, A. Mandlekar, B. Babich, G. State, M. Hutter, and A. Garg, “Orbit: A unified simulation framework for interactive robot learning environments,” *IEEE Robotics and Automation Letters*, vol. 8, pp. 3740–3747, 2023.
- [11] M. Quigley, K. Conley, B. Gerkey, J. Faust, T. Foote, J. Leibs, R. Wheeler, and A. Y. Ng, “Ros: an open-source robot operating system,” in *ICRA workshop on open source software*, vol. 3. Kobe, Japan, 2009, p. 5.
- [12] M. Walter, S. Karaman, E. Frazzoli, and S. Teller, “Closed-loop pallet manipulation in unstructured environments,” in *2010 IEEE/RSJ International Conference on Intelligent Robots and Systems (IROS)*, 2010.
- [13] S. Teller, M. Walter, M. Antone, A. Correa, R. Davis, L. Fletcher, E. Frazzoli, J. Glass, J. How, A. Huang, J. Jeon, S. Karaman, B. Luders, N. Roy, and T. Sainath, “A voice-commandable robotic forklift working alongside humans in minimally-prepared outdoor environments,” in *2010 IEEE International Conference on Robotics and Automation (ICRA)*, 2010, pp. 526–533.
- [14] S. Hadwiger and T. Meisen, “Autonomous load carrier approaching based on deep reinforcement learning with compressed visual information,” in *2022 5TH International Conference on Artificial Intelligence for Industries, AI4I*, 2022, pp. 48–53.
- [15] J. Fu, A. Kumar, O. Nachum, G. Tucker, and S. Levine, “D4rl: Datasets for deep data-driven reinforcement learning,” *arXiv preprint arXiv:2004.07219*, 2020.
- [16] F. Schmalstieg, D. Honerkamp, T. Welschehold, and A. Valada, “Learning hierarchical interactive multi-object search for mobile manipulation,” *IEEE Robotics and Automation Letters*, vol. 8, pp. 8549–8556, 2023.
- [17] V. Wiberg, E. Wallin, A. Fälldin, T. Semberg, M. Rossander, E. Wadbro, and M. Servin, “Sim-to-real transfer of active suspension control using deep reinforcement learning,” *Robotics and Autonomous Systems*, vol. 179, 2024.
- [18] E. Su, C. Jia, Y. Qin, W. Zhou, A. Macaluso, B. Huang, and X. Wang, “Sim2real manipulation on unknown objects with tactile-based reinforcement learning,” in *2024 IEEE International Conference on Robotics and Automation (ICRA)*, 2024, pp. 9234–9241.
- [19] I. Kostrikov, D. Yarats, and R. Fergus, “Image augmentation is all you need: Regularizing deep reinforcement learning from pixels,” *arXiv preprint arXiv:2004.13649*, 2020.
- [20] F. Sadeghi and S. Levine, “CAD²RL: Real single-image flight without a single real image,” in *Robotics: Science and Systems XIII*, 2017.
- [21] S. James, P. Wohlhart, M. Kalakrishnan, D. Kalashnikov, A. Irpan, J. Ibarz, S. Levine, R. Hadsell, and K. Bousmalis, “Sim-to-real via sim-to-sim: Data-efficient robotic grasping via randomized-to-canonical adaptation networks,” in *Proceedings of the IEEE/CVF conference on computer vision and pattern recognition*, 2019, pp. 12 627–12 637.
- [22] D. Tirumala, M. Wulfmeier, B. Moran, S. Huang, J. Humplik, G. Lever, T. Haarnoja, L. Hasenclever, A. Byravan, N. Batchelor *et al.*, “Learning robot soccer from egocentric vision with deep reinforcement learning,” *arXiv preprint arXiv:2405.02425*, 2024.
- [23] B. Mildenhall, P. P. Srinivasan, M. Tancik, J. T. Barron, R. Ramamoorthi, and R. Ng, “Nerf: Representing scenes as neural radiance fields for view synthesis,” *Communications of the ACM*, vol. 65, no. 1, pp. 99–106, 2021.
- [24] A. Byravan, J. Humplik, L. Hasenclever, A. Brussee, F. Nori, T. Haarnoja, B. Moran, S. Bohez, F. Sadeghi, B. Vujatovic, and N. Heess, “Nerf2real: Sim2real transfer of vision-guided bipedal motion skills using neural radiance fields,” in *2023 IEEE International Conference on Robotics and Automation (ICRA)*, 2023, pp. 9362–9369.
- [25] NVIDIA, “Isaac Sim - Robotics Simulation and Synthetic Data Generation.” [Online]. Available: <https://developer.nvidia.com/isaac-sim>
- [26] Q. Yu, M. Moghani, K. Dharmarajan, V. Schorp, W. C. H. Panitch, J. Liu, K. Hari, H. Huang, M. Mittal, K. Goldberg, and A. Garg, “Orbit-surgical: An open-simulation framework for learning surgical augmented dexterity,” in *2024 IEEE International Conference on Robotics and Automation (ICRA)*, 2024, pp. 15 509–15 516.
- [27] K. He, X. Zhang, S. Ren, and J. Sun, “Deep residual learning for image recognition,” in *Proceedings of the IEEE Conference on Computer Vision and Pattern Recognition (CVPR)*, June 2016.
- [28] J. Deng, W. Dong, R. Socher, L.-J. Li, K. Li, and L. Fei-Fei, “Imagenet: A large-scale hierarchical image database,” in *2009 IEEE conference on computer vision and pattern recognition*. IEEE, 2009, pp. 248–255.
- [29] R. Shah and V. Kumar, “Rrl: Resnet as representation for reinforcement learning,” in *International Conference on Machine Learning*. PMLR, 2021.
- [30] J. Schulman, F. Wolski, P. Dhariwal, A. Radford, and O. Klimov, “Proximal policy optimization algorithms,” *arXiv preprint arXiv:1707.06347*, 2017.
- [31] F. Xue, Y. Chang, T. Wang, Y. Zhou, and A. Ming, “Indoor obstacle discovery on reflective ground via monocular camera,” *International Journal of Computer Vision*, vol. 132, no. 3, pp. 987–1007, 2024.
- [32] LESU Model Technology Co., Ltd., “Lesu - manufacturer specialized in manufacturing simulation models.” [Online]. Available: <https://www.rclesu.com/>
- [33] D. Makoviichuk and V. Makoviychuk, “rl-games: A high-performance framework for reinforcement learning,” May 2021. [Online]. Available: <https://github.com/Denys88/rl-games>
- [34] NVIDIA, “Omniverse isaac gym reinforcement learning environments for isaac sim,” 2022. [Online]. Available: <https://github.com/isaac-sim/OmniIsaacGymEnvs>